

# CHARACTERISTICS OF DRIZZLING AND NON-DRIZZLING STRATOCUMULUS AS REVEALED BY VERTICAL POINTING CLOUD RADAR AND LIDAR

Ewan J. O'Connor<sup>1</sup>, Robin Hogan<sup>1</sup>, Anthony Illingworth<sup>1</sup> and Jean-Louis Brenguier<sup>2</sup>

<sup>1</sup>Department of Meteorology, University of Reading, Reading, Berkshire, United Kingdom

<sup>2</sup>Centre National de Recherches Météorologiques, Toulouse, France

## 1 INTRODUCTION

Both climate and operational forecasting models have difficulty representing stratocumulus and predicting their persistence and break-up. Typically the prognostic variables used to represent them in models are liquid water content and fractional cloud cover, in some climate models there is an implicit cloud droplet concentration via the prognostic aerosol variable. As part of the EU CloudNET project we will compare the values of the stratocumulus cloud parameters held in four operational models (ECMWF, Met Office, MeteoFrance and RACMO) with simultaneous observations of the vertical profile of the clouds with cloud radar and lidar at three observing sites: Chilbolton (UK), Cabauw (NL) and SIRTa, Paris, (France). The drizzle process is intimately linked to stratocumulus; observations (Miller *et al.*, 1998; Albrecht, 1989) and modelling studies (Albrecht, 1993; Wood, 2000) have shown that drizzle is important principally because it is involved in determining the cloud lifetime and evolution. The drizzle process may also have implications for the radiative properties of such clouds (Feingold *et al.*, 1996, 1997) through alteration of the cloud droplet spectra.

The techniques used to derive the microphysical parameters from the radar and lidar profiles are outlined in section 2 and some preliminary observations are shown in section 3.

## 2 TECHNIQUES

In this section we introduce two techniques to retrieve drizzle droplet and cloud droplet concentrations from millimeter-wave cloud radar and lidar data available at 30 s and 60 m resolution.

### 2.1 Drizzle droplet concentration

The technique detailed in O'Connor *et al.* (2004) combines Doppler radar measurements with those of a backscatter lidar to derive the microphysical properties of drizzle and can be applied to drizzle falling below cloud base. In-cloud measurements are not possible using this technique as the lidar beam is strongly attenuated as soon as it penetrates the cloud.

Corresponding author address: Ewan J. O'Connor, Department of Meteorology, University of Reading, Earley Gate, PO Box 243, Reading RG6 6BB, UK; E-mail: E.J.OConnor@reading.ac.uk.

The ratio of the radar to lidar backscatter power is proportional to the fourth power of mean size so potentially can provide an accurate size estimate and is insensitive to air motion. Once the size is known, the concentration can be derived from the observed radar reflectivity. The inferred drizzle droplet concentration and mean size are refined further by using the Doppler spectral width to infer the shape of the droplet size distribution given by the value of  $\mu$  when the size spectrum is fitted to a gamma function. Vertical profiles of drizzle parameters such as liquid water content, liquid water flux and the theoretical Doppler velocity that would be measured in still air can then be calculated for the derived size distribution and, because the absolute value of the mean Doppler velocity is not used in the retrieval of the drizzle droplet size distribution, the air vertical velocity can be inferred. This technique has the potential to retrieve vertical profiles of the median equivolumetric diameter ( $D_0$ ) of the drop size distribution, drizzle liquid water content and drizzle liquid water flux below cloud base to within 15%. The spatial scales of updrafts and downdrafts can also be derived and it was found that updrafts tended to coincide with the occurrence of the strongest drizzle streaks. When total liquid water path is available from microwave radiometers, the timescale for the depletion of cloud water by drizzle may also be estimated and observations suggest that this timescale varies from a few days in light drizzle to a few hours in strong drizzle events.

### 2.2 Cloud droplet concentration - drizzle free cloud

The adiabatic liquid water content is the theoretical maximum cloud liquid water content for a rising parcel. If liquid water clouds follow adiabatic processes and there is no entrainment then the observed liquid water profile should follow the adiabatic liquid water profile. The total water mixing ratio,  $q_t = q + q_l$ , where  $q$  is water vapour mixing ratio and  $q_l$  is liquid water mixing ratio, is assumed to be conserved during pseudo-adiabatic motion. Profiles of  $q_l$  under adiabatic conditions can be calculated in an iterative manner, given the temperature and pressure at cloud base, using the equation for  $dq_l/dz$  (e.g. Brenguier, 1991), the equation for the saturated adiabatic lapse rate and the hydrostatic equation. The value of  $dq_l/dz$  is approximately constant for shallow clouds (depth < 1 km) and the variation with temperature is shown in figure 1.

The adiabatic cloud profile for low level liquid water

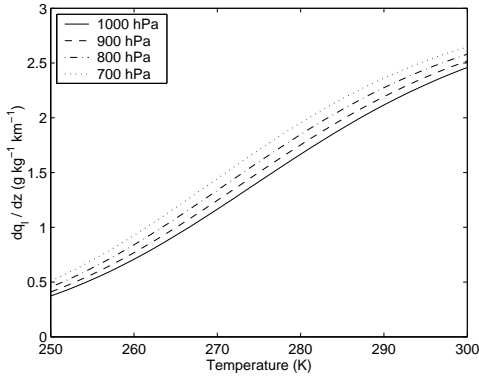


Figure 1: Variation of  $\frac{dq_l}{dz}$  with temperature at four different pressures.

clouds is therefore assumed to be adequately described by a linear increase of liquid water content, LWC, with height, which we define as

$$a = \frac{d(q_l \rho_a)}{dz} = \frac{dLWC}{dz}, \quad (1)$$

where  $\rho_a$  is the density of the air, assuming that there is no entrainment, and studies have suggested (Slingo *et al.*, 1982; Nicholls, 1984; Davidson *et al.*, 1984) that the number concentration of water droplets remains relatively constant throughout the profile. In reality, the profile of LWC does not necessarily follow the theoretical adiabatic profile and can contain values of LWC that are significantly lower than the adiabatic value. The process of entrainment can significantly reduce LWC, especially at cloud top.

Vertical profiles of LWC, droplet number concentration,  $N$ , and mean droplet diameter,  $D$ , derived from aircraft spectra collected during the ACE-2 CLOUDYCOLUMN closure experiment were presented in Brenguier *et al.* (2000a) for a marine and a polluted case and illustrate typical features, namely (i) that LWC follows the adiabatic profile close to cloud base, while its variability increases toward the top, due to entrainment and mixing with dry air; (ii) that  $N$  shows constant peak values throughout the cloud depth and varies in correlation with LWC; (iii) that  $D$  increases continuously from the base to the top, and that it does not show the same variability as LWC and  $N$  (Pawlowska and Brenguier, 2000). The slight variability of  $N$  at cloud base is attributed to the response of the cloud condensation nuclei activation process to variations in the vertical velocity (Snider and Brenguier, 2000). In the upper cloud levels, the fact that LWC variations are only reflected in variations of  $N$ , while  $D$  is not affected, is typical of a heterogeneous mixing process (Baker *et al.*, 1980), where it is assumed that turbulent mixing occurs on longer time-scales than that for droplet evaporation so that droplets of all sizes in an entrained subsaturated region of air evaporate completely while those in unmixed air remain the same size. The maximum  $N$  value is referred to as the adiabatic value,  $N_{ad}$ , and it is determined at cloud base by the CCN hygro-

scopic properties and the intensity of the updraft at cloud base.

Based on these observations, we can now make the following assumptions.

(i) In an undiluted cloud column, LWC increases linearly with height, according to the adiabatic model, with a value of  $a$ , defined in (1), that can be reliably estimated at cloud base using temperature and humidity profiles from a radiosonde or a model. The droplet concentration is constant in the cloud column, but its value  $N_{ad}$  is unknown. We assume a monodispersed distribution for simplicity, which implies that the radar reflectivity  $Z = ND^6$  and

$$LWC_{ad} = \rho_l \frac{\pi}{6} N_{ad} D_{ad}^3, \quad (2)$$

where  $\rho_l$  is the density of liquid water and the subscript (ad) refers to the theoretical adiabatic values.

(ii) In a diluted cloud column, the ratio of LWC to its adiabatic value is represented by the coefficient  $k$ , so that at some height  $z$ ,  $LWC(z) = k LWC_{ad}(z)$ . The assumption of inhomogeneous mixing postulates that  $N = k N_{ad}$  while  $D^3 = D_{ad}^3$  so that (2) can be written in terms of  $D$  as

$$D^3 = D_{ad}^3 = \frac{6}{\rho_l \pi} \frac{LWC_{ad}}{N_{ad}}, \quad (3)$$

and by substituting  $N = k N_{ad}$  and (3) into  $Z = ND^6$  we obtain

$$Z = k N_{ad} \left( \frac{6}{\rho_l \pi} \frac{LWC_{ad}}{N_{ad}} \right)^2. \quad (4)$$

Since  $a$  is effectively constant,  $LWC_{ad}(z) = az$ , where  $z$  refers to the height above cloud base, and (4) can be written as

$$Z(z) = \frac{36}{\rho_l^2 \pi^2} \frac{k (az)^2}{N_{ad}} \quad (5)$$

so that  $dZ/dz^2 \propto k/N_{ad}$ . A linear relationship between  $Z$  and  $z^2$  within a profile is expected and would validate the assumption of a profile of constant  $N$ .

The value of  $N_{ad}$  is taken from the peak value of the distribution of  $N$  over a suitable time period and the dilution factor,  $k$ , is then derived for each profile. The profiles of LWC and  $D$  can now be derived from the reflectivity values using (4) and (3). By using  $dZ/dz^2$  to derive  $N_{ad}$  and  $D_{ad}$  we have however introduced an additional assumption, namely that the dilution ratio  $k$  is constant over the portion of cloud depth examined to derive the slope  $dZ/dz^2$ .

The technique is only applicable in the absence of drizzle since any drizzle droplets within a profile can dominate the radar return, even at low concentrations, because of their larger size and distort the reflectivity profile so that  $dZ/dz^2$  is no longer proportional to  $k/N_{ad}$ . Since the lidar is not as sensitive to variations in size as the radar, drizzle droplets do not swamp the return from the much higher number concentration of cloud droplets. Any significant radar return below the cloud base detected by

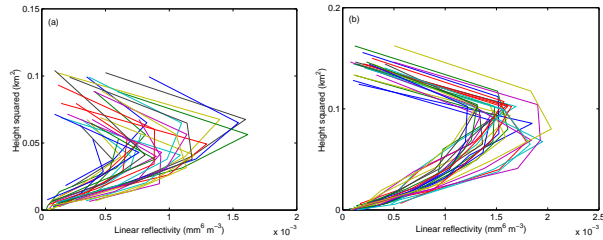


Figure 2: Profiles of linear reflectivity values versus height squared for two fifteen minute periods, (a) beginning at 1005 UTC and (b) beginning at 1545 UTC, on 5 July 2003.

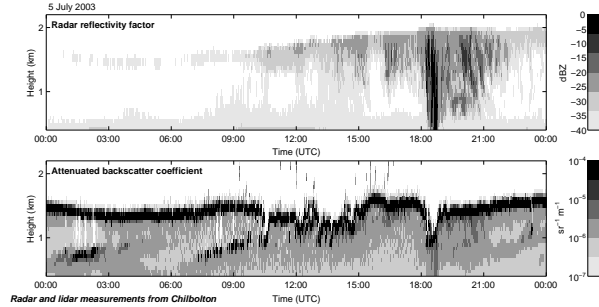


Figure 3: Observed variables for 5 July 2003. Time-height plots of (top panel) radar reflectivity factor, (lower panel) attenuated lidar backscatter.

the lidar will indicate if there is drizzle present and individual profiles are diagnosed as containing drizzle if  $Z$  is greater than  $-30$  dBZ 120 metres (two range gates) below the lidar cloud base.

### 3 OBSERVATIONS

To test the assumption that the number concentration  $N$  within a vertical profile remains constant we first examine reflectivity profiles in drizzle free stratocumulus to determine whether they conform to the assumption of  $Z \propto z^2$ . Profiles of  $Z$  vs  $z^2$  for 30 profiles taken every 30 seconds with 60 m vertical resolution over a 15 minute period are plotted in figure 2 and it can be seen that the assumption of  $Z \propto z^2$ , where  $z$  refers to the height above cloud base (the lidar is used to determine  $z = 0$  accurately), is valid in the lower region above cloud base for all profiles. The departure from the idealised  $Z \propto z^2$  profile occurs towards the top of the cloud and may be attributed to the process of entrainment due to radiatively driven overturning. The two occasions were chosen to correspond to profiles at different times of the day but both display similar characteristics. The minimum gradient represents adiabatic conditions ( $k = 1$ , no dilution) and steeper gradients are associated with  $k < 1$ , indicating that some dilution has occurred.

Figure 3 contains 24 hours of radar and lidar data taken on 5 July 2003 which displays a variety of cloud conditions. The low level cloud is characterised in the lidar data by a strong signal near cloud base throughout the day whereas the radar reflectivity is much more varied. Drizzle is present between 1620 and 2200 UTC

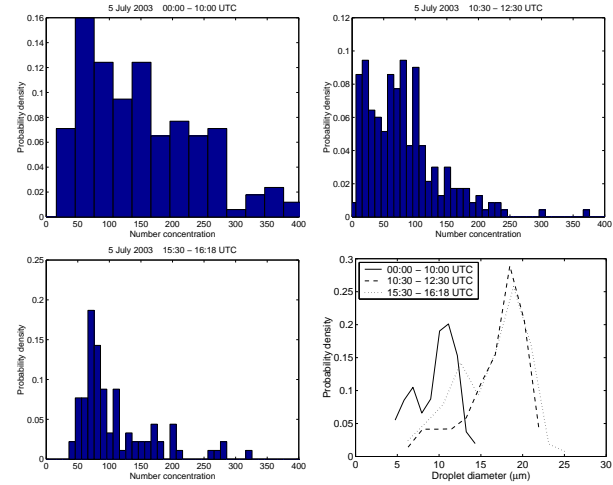


Figure 4: Frequency distributions of the droplet number concentration for three periods, (a) between 0000 and 1000 UTC, (b) between 1030 and 1230 UTC and (c) between 1530 and 1618 UTC, on 5th July 2003. (d) shows the frequency distribution of droplet diameter for the three periods.

(and intermittently between 1300 and 1500 UTC) producing the high radar reflectivity values up to  $-5$  dBZ. The temperature and pressure at cloud base were provided by the 0–6 hr forecast output of the Meteorological Office Unified Model for the grid point centred over Chilbolton and the theoretical adiabatic value of  $a$  for each profile was calculated. Figure 4 consists of frequency distributions of the droplet number concentration for three periods during the day shown in figure 3. Figure 4a corresponds to the period between 0000 and 1000 UTC where the cloud reflectivity is variable and often falls below the detection threshold of the radar. The value of  $N_{ad}$  for this time period is  $264 \text{ cm}^{-3}$  which is indicative of a polluted air mass and the distribution of  $N$  is very broad.

The second period encompasses reflectivities above the detection threshold prior to the onset of light drizzle with  $N_{ad} = 91 \text{ cm}^{-3}$  and the third period is just before the onset of heavy drizzle and is characterised by a narrow distribution with  $N_{ad} = 82 \text{ cm}^{-3}$ . These two cases are more representative of marine air masses and the shape of these two distributions are similar to those observed by Brenguier *et al.* (2000b) for this air mass type.

The droplet diameter from these periods can be inferred from the radar reflectivity factor and figure 4d shows the frequency distributions of the droplet diameter for the three time periods, including data from all heights within the profile. The first period between 0000 and 1000 UTC has inferred droplet diameters less than  $12 \mu\text{m}$  whereas the two periods which occur just prior to the onset of drizzle have larger diameters in the region of about  $18 \mu\text{m}$ . The critical droplet diameter for production of drizzle is usually estimated to be about  $10 \mu\text{m}$  (Trioli and Cotton, 1980) which is consistent with the values obtained here.

Figure 5 shows two of the drizzle parameters derived

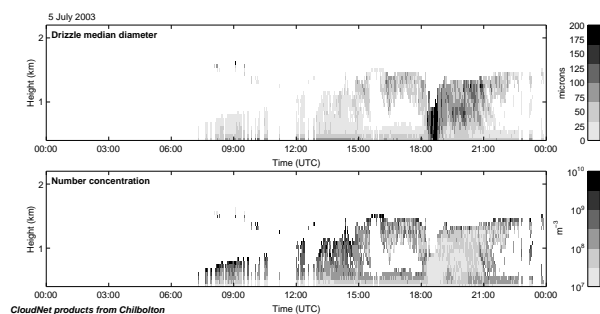


Figure 5: Derived drizzle variables for 5 July 2003. Time-height plots of (top panel) drizzle median equivolumetric diameter ( $D_0$ ), (lower panel) drizzle number concentration.

from the drizzle technique, drizzle diameter and drizzle number concentration, for profiles containing drizzle on the same day, 5th July 2003. The drizzle between 1300 and 1500 UTC is characterised by small sizes and high number concentration whereas the drizzle droplet size increases appreciably just after 1618 UTC. The cloud droplet mean size distributions prior to these two periods are relatively similar, as are the values of  $N_{ad}$ , although the distribution of cloud droplet number concentration is different, and implies that the shape of the cloud droplet size distribution plays a role in determining the amount of drizzle (a wider droplet size distribution will have a greater number of large drops for the same mean size). This information is crucial to parameterize the autoconversion process in models correctly. After 1800 UTC the drizzle droplet size increases dramatically while the concentration decreases by an order of magnitude as a result of coalescence and collision.

#### 4 DISCUSSION

The technique described in this paper shows potential for the retrieval of the vertical profile of various microphysical parameters. The values of droplet number concentration, liquid water content and droplet size are consistent with earlier researchers as is the variability encountered. The CloudNET project will provide the data to compare a long time series of data and relate cloud drop concentration and size to drizzle drop concentration and size to improve parametrization of the autoconversion process in models.

#### ACKNOWLEDGEMENTS

We are grateful to the Radiocommunications Research Unit at the Rutherford Appleton Laboratory for providing the radar data. This research was funded by NERC grant NER/T/S/1999/00105 and EU CloudNet contract EVK2-CT-2000-00065.

#### REFERENCES

Albrecht, B. A. (1989). Aerosols, cloud microphysics, and fractional cloudiness. *Science*, **245**, 1227–1230.

Albrecht, B. A. (1993). The effects of precipitation on the thermodynamic structure of trade-wind boundary layers. *J. Geophys. Res.*, **98**, 7327–7337.

Baker, M. B., Corbin, R. G., and Latham, J. (1980). The influence of entrainment on the evolution of cloud droplet spectra: (I). a model of inhomogeneous mixing. *Q. J. R. Meteorol. Soc.*, **106**, 581–598.

Brenguier, J.-L. (1991). Parameterization of the condensation process: A theoretical approach. *J. Atmos. Sci.*, **48**(2), 2724–2735.

Brenguier, J.-L., Chuang, P. Y., Fouquart, Y., Johnson, D. W., Parol, F., Pawlowska, H., Pelon, J., Schüller, L., Schröder, F., and Snider, J. (2000a). An overview of the ACE-2 CLOUDY-COLUMN closure experiment. *Tellus*, **52B**, 815–827.

Brenguier, J.-L., Pawlowska, H., Schüller, L., Preusker, R., Fischer, J., and Fouquart, Y. (2000b). Radiative properties of boundary layer clouds: Droplet effective radius versus number concentration. *J. Atmos. Sci.*, **57**(6), 803–821.

Davidson, K. L., Fairall, C. W., Boyle, P. J., and Scacher, G. E. (1984). Verification of an atmospheric mixed-layer model for a coastal region. *J. Climate Appl. Meteorol.*, **23**(4), 617–636.

Feingold, G., Stevens, B., Cotton, W. R., and Frisch, A. S. (1996). The relationship between drop in-cloud residence time and drizzle production in numerically simulated stratocumulus clouds. *J. Atmos. Sci.*, **53**(8), 1108–1122.

Feingold, G., Boers, R., Stevens, B., and Cotton, W. R. (1997). A modeling study of the effect of drizzle on cloud optical depth and susceptibility. *J. Geophys. Res. - Atmos.*, **102**(D12), 13527–13534.

Miller, M. A., Jensen, M. P., and Clothiaux, E. E. (1998). Diurnal cloud and thermodynamic variations in the stratocumulus transition regime: A case study using in situ and remote sensors. *J. Atmos. Sci.*, **55**, 2294–2310.

Nicholls, S. (1984). The dynamics of stratocumulus: Aircraft observations and comparisons with a mixed layer model. *Q. J. R. Meteorol. Soc.*, **110**, 783–820.

O'Connor, E. J., Hogan, R. J., and Illingworth, A. J. (2004). Retrieving stratocumulus drizzle parameters using doppler radar and lidar. *J. Appl. Meteorol.*, in press.

Pawlowska, H. and Brenguier, J.-L. (2000). Microphysical properties of stratocumulus clouds during ACE-2. *Tellus*, **52B**, 868–887.

Slingo, A. S., Nicholls, S., and Schnetz, J. (1982). Aircraft observations of marine stratocumulus during JASIN. *Q. J. R. Meteorol. Soc.*, **108**, 833–856.

Snider, J. R. and Brenguier, J.-L. (2000). Cloud condensation nuclei and cloud droplet measurements during ACE-2. *Tellus*, **52B**, 828–842.

Tripoli, G. J. and Cotton, W. R. (1980). A numerical investigation of several factors contributing to the observed variable intensity of deep convection over south Florida. *J. Appl. Meteorol.*, **19**, 1037–1063.

Wood, R. (2000). Parametrization of the effect of drizzle upon the droplet effective radius in stratocumulus clouds. *Q. J. R. Meteorol. Soc.*, **126**, 3309–3324.